High-efficiency carrier multiplication through direct photogeneration of multi-excitons via virtual single-exciton states

RICHARD D. SCHALLER[1], VLADIMIR M. AGRANOVICH[2,3] AND VICTOR I. KLIMOV[1]*

[1]Chemistry Division, Los Alamos National Laboratory, Los Alamos, New Mexico 87545, USA
[2]Institute of Spectroscopy, Russian Academy of Sciences, Troitsk, Moscow obl. 142190, Russia
[3]UTD-NanoTech Institute, The University of Texas at Dallas, Richardson, Texas 75083, USA
*e-mail: klimov@lanl.gov

Published online: 13 November 2005; doi:10.1038/nphys151

We have previously demonstrated that absorption of a single photon by a nanocrystal quantum dot can generate multiple excitons with an efficiency of up to 100%. This effect, known as carrier multiplication, should lead to substantial improvements in the performance of a variety of optoelectronic and photocatalytic devices, including solar cells, low-threshold lasers and entangled photon sources. Here we present detailed analysis of the dynamics that govern the ultrafast growth of multi-exciton populations in CdSe and PbSe nanocrystals and propose a model of how such populations arise. Our analysis indicates that the generation of multi-excitons in these systems takes less than 200 fs, which suggests that it is an instantaneous event. We explain this in terms of their direct photogeneration via multiple virtual single-exciton states. This process relies on both the confinement-enhanced Coulomb coupling between single excitons and multi-excitons and the large spectral density of high-energy single- and multi-exciton resonances that occur in semiconductor nanocrystals.

Solar cells represent an important clean source of energy. However, to make them competitive with traditional energy sources, the cost/efficiency ratio must be reduced appreciably. Cost considerations have been a strong driver for the development of non-silicon photovoltaic devices that are instead based on, for example, polymers (plastic cells)[1] and dye-sensitized porous metal oxides (Grätzel cells)[2]. Increases in efficiency have typically relied on iterative improvements in material quality (for both Si and non-Si systems) and/or device engineering aspects including, for example, the use of tandem architectures. There exist, however, approaches that can potentially lead to leaps in photovoltaic performance through the use of different principles for conversion of solar energy into electricity. One such approach involves the use of carrier multiplication (CM) for increasing the photocurrent of solar cells[3–7].

CM is very efficient in quantum-confined semiconductor nanocrystals, whereas it is inefficient in bulk semiconductors (the maximum CM-induced increase in the efficiencies of traditional solar cells is less than 1%; ref. 8). By analysing dynamical signatures of excitons and multi-excitons in PbSe nanocrystals, we discovered that the absorption of a single photon can produce two or even three electron–hole pairs (excitons), which results in internal quantum efficiencies (QEs) greater than 200% for conversion of light quanta into charge carriers[9]. These results were confirmed in ref. 10 in similar studies of PbSe nanocrystals and nanocrystals of another lead salt compound, PbS. We have extended the photon energies further to the ultraviolet and achieved nearly complete filling of the lowest eight-fold degenerate 1S quantized state in PbSe nanocrystals by a single-photon absorption event. Furthermore, we also detected high-CM efficiencies (QE up to 165%) in CdSe nanocrystals, which are characterized by energy structures and carrier dynamics that are distinctly different from those of the lead salt nanocrystals[11]. These experimental observations are difficult to reconcile in the traditional CM mechanism of impact ionization[3–7],

©2005 Nature Publishing Group

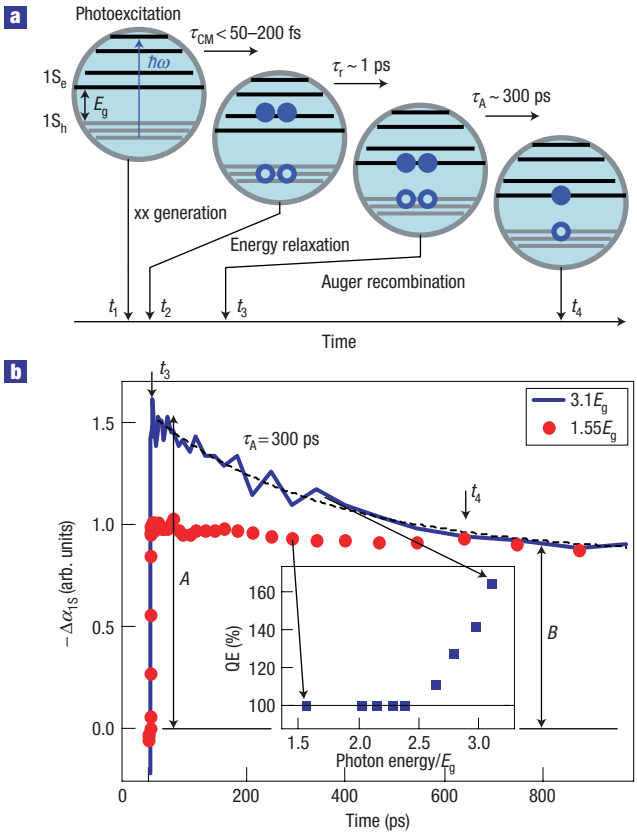

Figure 1 Evolution of the electron–hole system when photoexcited in the regime of CM. a, Schematics of generation/relaxation processes in a nanocrystal following excitation with an ultrashot laser pulse with a photon energy that is sufficient to produce CM. Absorption of a photon (at time t_1) with energy greater than the CM threshold results in the generation of a 'hot' bi-exciton (at time t_2) on the timescale of τ_{CM}. After relaxing to its ground state (at time t_3) with the sub-picosecond time constant τ_r, this bi-exciton recombines on the sub-nanosecond timescale (time constant τ_A) by the non-radiative Auger process to produce a single exciton (at time t_4). Finally, the exciton recombines radiatively on a much slower timescale of tens to hundreds of nanoseconds. A significant difference in the relaxation behaviour of bi-excitons (fast decay) and single excitons (slow decay) is the key property of nanocrystals that allowed us for the first time to detect CM and to quantify its efficiency[9]. **b**, 1S bleaching dynamics with (thick solid line) and without (circles) CM in 3.2-nm-radius CdSe nanocrystals ($E_g = 2.0$ eV). The dashed line is a two-exponential fit that indicates the presence of the short-lived bi-excitonic component. Inset: CM QE in CdSe nanocrystals as a function of pump photon energy normalized by E_g.

which suggests that a different physical phenomenon is responsible for CM in nanocrystal materials.

To address the issue of the CM mechanism, here we report detailed studies of buildup dynamics of the multi-exciton population produced by CM in PbSe and CdSe nanocrystals. We observe that in both types of nanocrystals the populations of the lowest quantized states in the regime of CM develop with sub-picosecond to picosecond time constants that are consistent with timescales of intraband relaxation. We do not detect any additional time delays (with better than 50–200 fs accuracy) that could be attributed to the CM process itself, which strongly suggests that multi-excitons are generated instantaneously by a single absorbed photon. To explain this specific observation as well as the results of previous experiments[9–11], we propose a model that describes CM in terms of direct generation of multi-excitons via virtual single-exciton states. This mechanism of CM has never been considered previously in semiconductors and relies on confinement-enhanced Coulomb coupling between single- and multi-exciton states, which is a unique feature of ultrasmall semiconductor nanocrystals.

To study nanocrystal population dynamics, we use an ultrafast transient-absorption experiment. In this experiment, solutions of spherically shaped nanocrystals (produced according to established procedures[12,13]) are excited with sub-100-fs pump pulses of a variable photon energy ($\hbar\omega$, where $\hbar$ is the reduced Planck constant and ω is frequency), and pump-induced absorption change at the position of the lowest-energy 1S transition, $\Delta\alpha_{1S}$, is probed with a second ultrashort pulse with 50–200 fs duration depending on the laser wavelength (see Fig. 1a for a schematic representation of the evolution of the electron–hole system following excitation by an ultrashort laser pulse). In all CM measurements, we use low excitation fluences (nominally less than 0.1 exciton per nanocrystal was excited on average) to reduce the effect of direct generation of multi-excitons by absorption of multiple photons. Under this condition, multiple excitons are primarily produced through CM, and the average exciton multiplicity in photoexcited nanocrystals, $\langle N_x \rangle$, immediately following the pump pulse can be derived from the ratio of the signal amplitude measured at short times after excitation (A) to the long-lived, single-exciton background (B): $\langle N_x \rangle = A/B$ (see Fig. 2a and the detailed experimental procedures in Methods). Finally, QE for conversion of light quanta into excitons can be calculated as QE = 100% $\langle N_x \rangle$.

In Fig. 1b, we compare the decay dynamics of the 1S transient-absorption signal in CdSe nanocrystals for excitation energies of $1.55E_g$ (circles) and $3.1E_g$ (solid line); E_g is the nanocrystal energy gap. Because of energy conservation, CM can only take place if the pump photon energy is at least $2E_g$. (The CM thresholds measured for CdSe and PbSe nanocrystals are $2.5E_g$ and $2.9E_g$, respectively. These values are higher than the energy-conservation-based limit of $2E_g$, because, in addition to the energy-conservation law, the CM process in nanocrystals should also satisfy some extra requirements such as, for example, optical selection rules.) Therefore, CM is not possible with $1.55E_g$ photons, although it can occur if the photon energy is $3.1E_g$. Indeed, the time transient measured using $3.1E_g$ photons clearly shows a fast 'bi-excitonic' component that is not present with $1.55E_g$. Furthermore, from the ratio of the signal amplitude to the long-lived background we determine a QE of 165%, which indicates that bi-excitons are generated in more than 50% of all photoexcited nanocrystals.

Despite the strong difference in relaxation behaviour, the transients measured at two different excitation energies show remarkably similar buildup dynamics (compare the circles and thick solid line in Fig. 2a). In the case of the $1.55E_g$ pump, the 1S transient-absorption signal buildup is controlled by the electron intraband relaxation[14]. Specifically, a final stage of the $\Delta\alpha_{1S}$ signal growth at time delay $\Delta t > 400$ fs is because of electron relaxation from the first-excited (1P) to the ground (1S) conduction-band state (complimentary 1P and 1S transient-absorption dynamics are shown in Fig. 2a by crosses and circles, respectively; see also the schematics of relaxation processes in Fig. 2b). The duration of the initial relaxation stage ($\Delta t < 400$ fs) is determined by the population buildup of the 1P level. The non-zero 1S signal at these early times, when the 1S state is not yet populated, arises from the Coulomb-interaction-induced shift of the lowest transition owing to hot carriers in high-energy states (the carrier-induced Stark effect)[14,15]. From the measured transient-absorption dynamics, we estimate that the average energy-loss rates during the initial (1P state population buildup) and the final (1S state population buildup) stages of intraband relaxation are 2.3 and 0.33 eV ps^{-1}, respectively. These values indicate that, despite a small 1P–1S

©2005 Nature Publishing Group

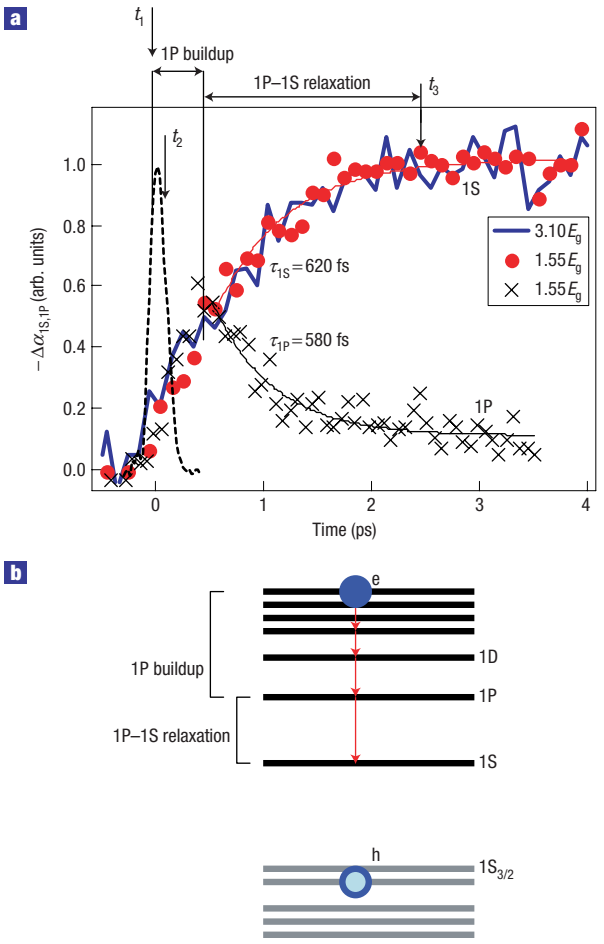

Figure 2 Buildup dynamics of the lowest 1S electron state in 3.2-nm-radius CdSe nanocrystals with and without CM (the same sample as in Fig. 1b). **a**, Transient-absorption dynamics measured at the positions of the 1S (circles, no CM; thick solid line, CM) and the 1P (crosses) transitions. Thin solid lines are exponential fits, which demonstrate that the 1S and the 1P population dynamics are complementary as expected for the 1P-to-1S relaxation. The dashed line is a pump–probe cross correlation. **b**, The schematics of intraband relaxation processes in CdSe nanocrystals. Arrows indicate sequential energy relaxation events during the descent of an electron from the initially excited state to the lowest 1S state. Two relaxation processes monitored in part **a** are highlighted by brackets: the population buildup of the 1P state (upper bracket) and the final stage of the 1P-to-1S relaxation (lower bracket).

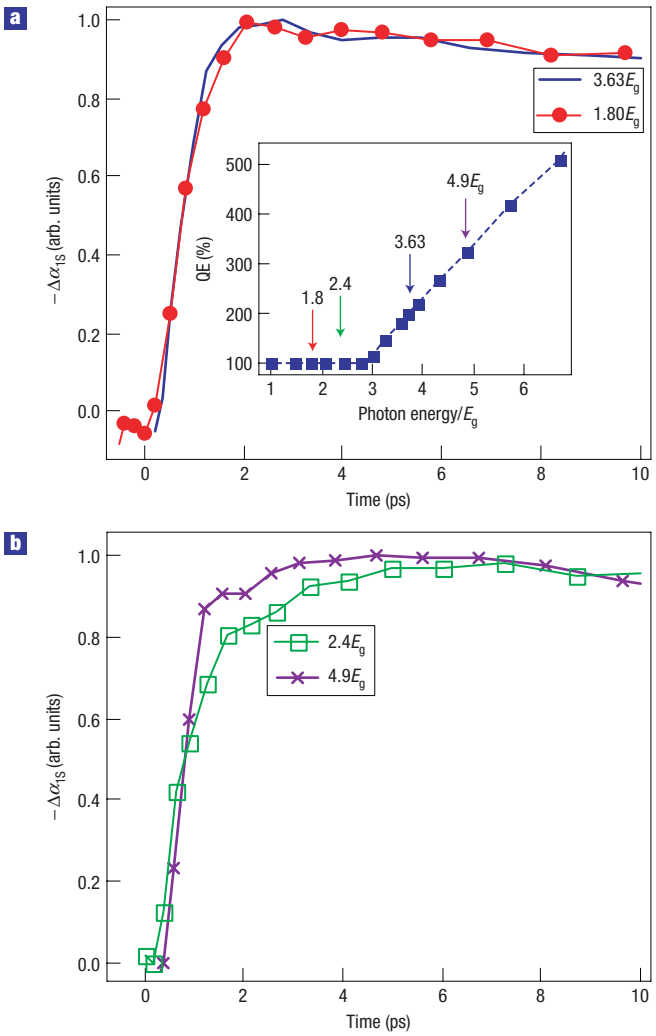

Figure 3 Buildup dynamics of the lowest 1S electron state in 3.9-nm-radius PbSe nanocrystals (E_g = 0.64 eV) with and without CM. a,**b**, The 1S buildup dynamics measured with pump photon energies of 1.8E_g (circles, no CM), 2.4E_g (squares, no CM), 3.63E_g (solid line, CM with QE = 200%) and 4.9E_g (crosses, CM with QE = 325%). Pump and probe pulse durations are ~50 fs. The inset in **a** is a plot of CM QE as a function of pump photon energy normalized by E_g (arrows mark the pump spectral positions used to record the dynamics shown in the figure).

separation (~200 meV), the relaxation between these two low-energy states is significantly slower than the relaxation at higher energies and, therefore, it provides a dominant contribution to the delay in the development of the 1S transient-absorption signal.

In the case of the 3.1E_g pump, the 1S signal buildup (the thick solid line in Fig. 2a) is characterized by similar ultrafast dynamics. Specifically, we observe that at $\Delta t > 400$ fs the time transients recorded using 1.55E_g and 3.1E_g pump photons closely follow each other, suggesting that the electron 1P-to-1S relaxation governs the late-stage $\Delta\alpha_{1S}$ buildup in the CM regime as in the no-CM case. This observation further suggests that CM can only occur within the initial 400 fs after excitation. In fact, the actual time of this process should be even shorter as we should take into account the fact that this buildup stage also includes the electron relaxation time from the initially photoexcited state to the 1P state. For example, in the case of the 3.1E_g pump photons, CM produces hot carriers with a per-exciton excess energy of ~0.9 eV relative to the 1P optical transition. The relaxation of this energy (given the energy-loss rate estimated above) will require approximately 400 fs, which is identical to the experimentally measured population buildup time of the 1P state. These considerations provide strong evidence that CM probably occurs on timescales that are shorter than our time resolution (50–200 fs depending on the probe wavelength).

A similar conclusion can be made on the basis of analysis of the 1S transient-absorption dynamics measured for PbSe nanocrystals. In Fig. 3a, we show transient-absorption time traces measured using pump photon energies of 1.80E_g and 3.63E_g that correspond to QEs of 100% (no CM) and 200%, respectively (see the inset in Fig. 3a). In the case of CM, carriers are produced with an excess energy of 0.82E_g per exciton, which is close to the excess energy in the no-CM case (0.8E_g). For both pump-photon energies, the 1S-state buildup dynamics are essentially identical, indicating that

©2005 Nature Publishing Group

they are controlled by the intraband relaxation process and that no additional (measurable) delay is introduced by the CM process. This point is further confirmed by the data in Fig. 3b, which shows two traces measured at $2.4E_g$ (QE = 100%) and $4.9E_g$ (QE = 325%). The excitation at $4.9E_g$ produces approximately three excitons per nanocrystal with excess energy of $\sim 0.6E_g$ per exciton, whereas this excess energy is $1.4E_g$ in the case of the $2.4E_g$ pump. Using energy-relaxation arguments one may expect faster 1S population buildup for the $4.9E_g$ pump despite greater pump-photon energy, which is indeed observed experimentally (compare the traces shown by crosses and squares in Fig. 3b). Thus, in the case of CM, the buildup of the 1S-state population is dominated by energy relaxation, as in the no-CM case. Furthermore, the time of this relaxation is determined not by the 'absolute' excess energy of the pump photon ($\hbar\omega - E_g$) but by the excess energy of the individual excitons comprising a multi-exciton state produced by CM (which is approximately $\hbar\omega/\langle N_x\rangle - E_g$). Therefore, the 1S-state buildup time can show non-monotonous behaviour with increasing pump photon energy as, for example, observed in Fig. 3b.

The above analysis of transient-absorption buildup dynamics indicates that CM takes place on extremely short timescales (shorter than 50–200 fs) and that it most probably occurs instantaneously. The instantaneous generation of multi-excitons, however, can be explained neither by a traditional impact ionization mechanism[3–7] nor by a proposed model of 'coherent evolution of a quantum state from the initial single exciton to a coherent superposition of multiple exciton states' (referred to as the coherent-CM model)[10]. In the impact ionization model, CM is the process that is inverse with respect to Auger recombination; therefore, it should be characterized by a time constant that is comparable to or even longer than that of the Auger decay[7,16]. Experimental data, however, indicate that the characteristic CM time is much shorter than the Auger-recombination time (tens to hundreds of picoseconds for Auger recombination[9,17] and sub-200 fs for CM), indicating that CM is probably not an Auger-type phenomenon.

In the model of coherent CM, the combined single-exciton/multi-exciton system is photoexcited through its single-exciton component and then experiences coherent oscillations between various resonant-exciton and multi-exciton states[10]. This mechanism can potentially lead to an oscillatory buildup of the multi-exciton population if the dephasing of the combined single-exciton/multi-exciton wavefunction occurs primarily via its multi-excitonic component. However, neither in our initial report[9] nor here do we resolve any well-defined oscillations in the buildup of the multi-exciton population in either PbSe or CdSe nanocrystals. These oscillations were also not detected in ref. 10, although the authors of this paper were explicitly looking for this effect. Instead, our data indicate that the 1S-state buildup is dominated by the intraband relaxation process, which further suggests that in both materials multi-excitons are generated instantaneously by the pump pulse.

To explain the experimental data that are now available for CM in nanocrystals[9–11], we propose a model of direct photogeneration of multi-excitons by a single photon via virtual, single-exciton states. This process can be explained in terms of second-order perturbation theory and is somewhat similar to the indirect ('non-vertical') optical transitions that occur in bulk semiconductor materials. For example, in silicon the band-edge transition couples the hole from the Γ valley to the electron in the X valley and, therefore, it cannot occur in first-order perturbation theory because of the momentum conservation requirement. However, it is allowed in second-order perturbation theory in which the coupling between different valleys is provided by the electron–phonon interaction hamiltonian (phonon-assisted transitions).

In a similar motif, in our model the electron–electron Coulomb interaction hamiltonian, H_{ee}, couples a virtual single-exciton state to a multi-exciton state. In this case, the transition probability for direct generation of a bi-exciton (the bi-exciton generation rate, W_2) by a single photon, $\hbar\omega$, can be presented as follows:

$$W_2 = \frac{2\pi}{\hbar}\sum_{xx}\left|\sum_{x}\frac{\langle 0|H_{e\gamma}|x\rangle\langle x|H_{ee}|xx\rangle}{\hbar\omega - E_x}\right|^2 \delta(\hbar\omega - E_{xx}), \qquad (1)$$

where $H_{e\gamma}$ is the hamiltonian of the electron–photon interaction that couples the nanocrystal ground state, $|0\rangle$, to a virtual single-exciton state, $|x\rangle$, and H_{ee} provides a coupling between the intermediate virtual exciton state and the final bi-exciton state, $|xx\rangle$ (Fig. 4a). E_x and E_{xx} are the energies of the single-exciton and the bi-exciton states, respectively. In second-order perturbation theory, energy conservation is required for the final state as expressed by the δ-function; however, it is not applicable to the virtual single-exciton states. Therefore, as indicated by the summation in equation (1), multiple single-exciton states can participate in the second-order transition by providing contributions that are weighted according to their proximity to the photon energy and the strength of their coupling to the optical field. As in the case of the coherent-CM model, our current approach relies on Coulomb coupling between single- and multi-exciton states; however, it considers a different limit of this coupling. Coherent CM would occur in the regime of strong coupling if the coupling constant were greater than the dephasing rate. In contrast, our perturbation approach describes the situation of weak to moderate coupling when dephasing dominates Coulomb interactions.

As photoexcitation above the nanocrystal energy gap can also produce single excitons, the efficiency of directly generating bi-excitons, η_{xx}, depends on the ratio of bi-exciton/single-exciton (W_1) generation rates, $f = W_2/W_1$, and can be expressed as $\eta_{xx} = f(1+f)^{-1}$, where W_1 is calculated as

$$W_1 = \frac{2\pi}{\hbar}\sum_{x}\left|\langle 0|H_{e\gamma}|x\rangle\right|^2\delta(\hbar\omega - E_x). \qquad (2)$$

Also, the QE for producing charge carriers by absorbed photons is QE = 100% $(1+\eta_{xx})$.

To roughly estimate the magnitude of the effect, below we perform calculations of CM efficiency taking into account a single bi-exciton state (located near the CM threshold) that is excited through a single, virtual exciton state, which is in the vicinity of the bi-exciton resonance (Fig. 4a). These calculations will underestimate the CM efficiency because, according to equation (1), in real systems multiple exciton and bi-exciton states will contribute to the probability W_2. Using equations (1) and (2) and introducing line shapes of the excitonic (g_x) and the bi-excitonic (g_{xx}) transitions (the respective widths are Γ_x and Γ_{xx}), we obtain the following simplified expression for f:

$$f(\hbar\omega) \approx \beta_{xx}^2 \frac{\Gamma_x^2}{(\hbar\omega - E_x)^2 + \Gamma_x^2}\frac{g_{xx}(\hbar\omega)}{g_x(\hbar\omega)}, \qquad (3)$$

where $\beta_{xx} = |\langle x|H_{ee}|xx\rangle|\Gamma_x^{-1}$ is a dimensionless parameter that determines the strength of the Coulomb coupling between the virtual single-exciton and the final bi-exciton states. According to equation (3), f is of the order of β_{xx}^2 in the vicinity of the CM threshold, which indicates that the rate of generation of bi-excitons can be a significant fraction of the single-exciton generation rate if the energy of the Coulomb interaction ($V_{xx} \approx |\langle x|H_{ee}|xx\rangle|$) is comparable to the exciton transition linewidth.

At present, there are no experimental data available for the strength of the exciton-to-bi-exciton Coulomb coupling in nanocrystals. However, one might expect that its magnitude

©2005 Nature Publishing Group

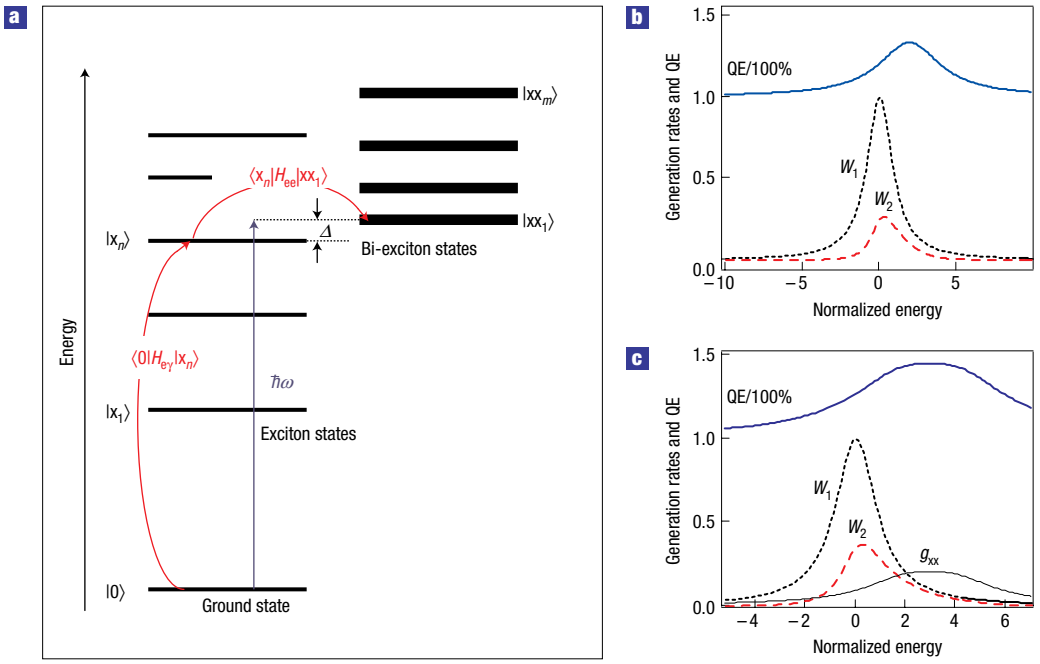

Figure 4 Direct photoexcitation of bi-excitons via virtual single-exciton states. a, Schematics of the second-order process in which the bi-exciton state $|xx_1\rangle$ is generated via Coulomb coupling to the virtual single-exciton state $|x_n\rangle$. **b**, Calculated single-exciton (W_1) and bi-exciton (W_2) generation rates along with corresponding QEs for the case of a single bi-exciton state excited via a single virtual exciton resonance. **c**, The same but for the case of two bi-exciton resonances excited via a single virtual exciton state; g_{xx} is the spectral density of the bi-exciton states. In both **b** and **c**, the horizontal axes are in terms of the normalized detuning, Δ/Γ_x.

is comparable to the energy of the Coulomb exciton–exciton interaction (the bi-exciton binding energy), which can be measured experimentally from, for example, energy separation between single-exciton and bi-exciton emission lines. Specifically, experiments on colloidal CdSe nanocrystals[18] indicate exciton–exciton interaction energies from 14 to 33 meV (depending on the nanocrystal size), which are much greater than the corresponding energies in bulk CdSe (4.5 meV; ref. 19). These values are comparable to linewidths of nanocrystal excited states (several tens of millielectronvolts as derived from single-nanocrystal studies[20]), indicating that confinement-enhanced Coulomb interactions in nanocrystals can lead to a significant probability of generating multi-excitons through coupling to virtual single-exciton states. On the other hand, because of significant broadening of high-energy electronic states in nanocrystals, the Coulomb coupling is probably not sufficiently strong to produce a coherent superposition of excitonic and multi-excitonic wavefunctions, as indicated by the lack of coherent oscillations in the buildup dynamics of multi-exciton populations. (Optical transitions in nanocrystals are often described in terms of narrow 'atomic-like' lines. This description is indeed applicable in the case of the lowest-energy, 'emitting' transition, which is narrow, of sub-millielectronvolt linewidth, at cryogenic temperatures. However, excitation of multi-excitons in the CM process occurs via high-energy excitonic resonances that are significantly broadened, tens of millielectronvolt and higher, by ultrafast intraband relaxation.)

To estimate the CM efficiencies that can be produced in the above approach, we use equations (1)–(3) to calculate the QE along with single- and bi-exciton generation rates using lorentzian line shapes for both the bi-excitonic and excitonic transitions (Fig. 4b) and assuming that $\Gamma_{xx} = 2\Gamma_x$. These calculations indicate that, even in the simple two-transition model, bi-excitons can be generated with high, tens of per cent, efficiencies (see the example in Fig. 4b, which demonstrates a QE of >130%) at relatively moderate strengths of Coulomb coupling ($\beta_{xx} = 1$). Furthermore, the proposed mechanism does not require precise resonance between single- and two-exciton states, and produces high bi-exciton generation rates at detunings (Δ) of up to a few transition linewidths.

So far, we have only considered the situation of a single virtual exciton state and a single bi-exciton transition. However, the proposed model can easily be generalized to the case of multiple transitions. Such generalization is actually essential to explain the continuous growth of CM efficiency above the CM threshold as well as to explain QE values greater than 200%. In Fig. 4c, we show the situation where two bi-exciton resonances (detunings $\Delta = 2\Gamma_x$ and $4\Gamma_x$) are excited via the same virtual single-exciton state. Owing to the presence of the second resonance, the range of the efficient bi-exciton generation extends further into the blue and QE increases up to more than 140%. It is also easy to demonstrate that the existence of extra higher-energy virtual single-exciton resonances will further boost the rate of multi-exciton production. Thus, in addition to enhanced Coulomb coupling, large densities of both high-energy single-exciton and multi-exciton transitions are essential for obtaining large CM QEs. Furthermore, the continuous increase of the CM efficiency with increasing pump-photon energy observed experimentally (the insets in Figs 1b and 3a) probably occurs because the growth of the density of the multi-exciton states outpaces the growth of the single-exciton density of states, which produces the overall increase of the g_{xx}/g_x factor (see equation (3)) with increasing $\hbar\omega$.

In conclusion, analysis of buildup dynamics of multi-exciton populations in CdSe and PbSe nanocrystals indicates that multi-excitons in the regime of CM are generated by single photons on an extremely short timescale (shorter than 50–200 fs) and in our experiments CM appears as an instantaneous event. To

©2005 Nature Publishing Group

explain this observation, we propose a model of direct generation of multi-excitons by a single absorbed photon via Coulomb coupling to virtual single-exciton states. This process relies on confinement-induced enhancement of Coulomb interactions in nanocrystals and large spectral densities of high-energy single-exciton and multi-exciton states.

METHODS

The pump-induced absorption change at the position of the lowest 1S transition, $\Delta\alpha_{1S}$, provides a measure of the total number of carriers occupying the 1S quantized state. In this work, we use low excitation intensities ($\langle N_0\rangle = j_p\sigma_a \ll 1$, where j_p is the per-pulse pump fluence and σ_a is the nanocrystal absorption cross-section), for which $\langle N_0\rangle$ is approximately equal to the fraction of photoexcited nanocrystals in the nanocrystal ensemble. Under this condition, multiple excitons are primarily produced by CM. In this case, the average exciton multiplicity in photoexcited nanocrystals, $\langle N_x\rangle$, and hence CM QE (QE = 100% $\langle N_x\rangle$), is determined not by the pump fluence but by the pump-photon energy[9]. One consequence of this phenomenon is that the maximal exciton multiplicity, $N_{x,max}$, in the nanocrystal ensemble is limited by $\hbar\omega/E_g$, which is a result of the energy conservation requirement. Furthermore, if $N_{x,max}$ is smaller than the 1S-state degeneracy (which is true for both CdSe and PbSe nanocrystals under our experimental conditions), then $\Delta\alpha_{1S}$ is simply proportional to $\langle N_x\rangle$: $\Delta\alpha_{1S} \propto \langle N_0\rangle\langle N_x\rangle$. Without CM and for low excitation intensity ($\langle N_0\rangle \ll 1$), $\langle N_x\rangle = 1$ and, therefore, the 1S transient-absorption dynamics are solely due to changes in the total number of photoexcited nanocrystals, which occurs by slow radiative decay characterized by time constants (τ_r) of tens (CdSe nanocrystals[21]) to hundreds of nanoseconds (PbSe nanocrystals[22,23]). In the presence of CM, the $\Delta\alpha_{1S}$ dynamics reflect changes in both $\langle N_0\rangle$ and the exciton multiplicity, $\langle N_x\rangle$. In nanocrystals, the dominant channel of the multi-exciton decay (and hence the decay of $\langle N_x\rangle$) is non-radiative Auger recombination, which occurs with picosecond to hundreds-of-picosecond time constants (τ_A); refs 9,17. Because of this difference of several orders of magnitude between τ_r and τ_A, at short times after excitation ($\Delta t \ll \tau_r$), the 1S transient-absorption signal decay is dominated by changes in multiplicity induced by Auger recombination, which produces a fast component in the transient-absorption signal. At $\Delta t \gg \tau_A$ (which corresponds to times longer than the duration of the fast transient-absorption component), all multi-excitons decay into single excitons and hence the corresponding multiplicity is then one: $\langle N_x\rangle(\tau_A \ll \Delta t \ll \tau_r) = 1$. Thus, the height of the long-lived background (B in Fig. 1b) in transient-absorption traces provides a calibration scale bar for deriving the exciton multiplicity produced by CM immediately after excitation: $\langle N_x\rangle(\Delta t \ll \tau_A) = A/B$, where A is the amplitude of the transient-absorption signal measured at short times after excitation (Fig. 1b).

The fast 1S transient-absorption component, which we use as a signature of CM, can, in principle, also be caused by trapping of 1S carriers at surface defects. However, this effect is insignificant in the samples studied in this work as indicated by the absence of the fast transient-absorption component in the case of excitation below the CM threshold. The processes leading to removal of carriers from excited electronic states (during, for example, nanocrystal ionization) are not manifested in 1S population dynamics and, therefore, they cannot significantly alter measured CM efficiencies. Furthermore, in our preliminary studies, absolute values of the pump-induced 1S absorption changes are not found to deviate significantly from what is expected from calculations based on absorption cross-section and excitation intensity even at high pump-photon energies. This result indicates that nanocrystal ionization is probably not efficient, at least in the range of pump-photon energies studied here. A possible reason for the low efficiency of ionization processes is that a single high-energy exciton may not ever exist following absorption of a high-energy photon, but instead multi-excitons composed of several low-energy excitons are excited directly (see the theory portion of this paper).

Received 15 July 2005; accepted 29 September 2005; published 13 November 2005.

References

1. Yu, G., Gao, J., Hummelen, J. C., Wudl, F. & Heeger, A. J. Polymer photovoltaic cells: Enhanced efficiencies via a network of internal donor-acceptor heterojunctions. *Science* **270,** 1789–1791 (1995).
2. Grätzel, M. Photoelectrochemical cells. *Nature* **414,** 338–344 (2001).
3. Landsberg, P. T., Nussbaumer, H. & Willeke, G. Band-band impact ionization and solar cell efficiency. *J. Appl. Phys.* **74,** 1451–1452 (1993).
4. Kolodinski, S., Werner, J. H., Wittchen, T. & Queisser, H. J. Quantum efficiencies exceeding unity due to impact ionization in silicon solar cells. *Appl. Phys. Lett.* **63,** 2405–2407 (1993).
5. Spirkl, W. & Ries, H. Luminescence and efficiency of an ideal photovoltaic cell with charge carrier multiplication. *Phys. Rev. B* **52,** 11319–11325 (1995).
6. Nozik, A. J. Quantum dot solar cells. *Physica E* **14,** 115–120 (2002).
7. Califano, M., Zunger, A. & Franceschetti, A. Direct carrier multiplication due to inverse Auger scattering in CdSe quantum dots. *Appl. Phys. Lett.* **84,** 2409–2411 (2004).
8. Wolf, M., Brendel, R., Werner, J. H. & Queisser, H. J. Solar cell efficiency and carrier multiplication in $Si_{1-x}Ge$ alloys. *J. Appl. Phys.* **83,** 4213–4221 (1998).
9. Schaller, R. D. & Klimov, V. I. High efficiency carrier multiplication in PbSe nanocrystals: Implications for solar energy conversion. *Phys. Rev. Lett.* **92,** 186601 (2004).
10. Ellingson, R. *et al.* Highly efficient multiple exciton generation in colloidal PbSe and PbS quantum dots. *Nano Lett.* **5,** 865–871 (2005).
11. Schaller, R. D., Petruska, M. A. & Klimov, V. I. The effect of electronic structure on carrier multiplication efficiency: A comparative study of PbSe and CdSe nanocrystals. *Appl. Phys. Lett.* (in the press).
12. Murray, C. B., Norris, D. J. & Bawendi, M. G. Synthesis and characterization of nearly monodisperse CdE (E = S, Se, Te) semiconductor nanocrystallites. *J. Am. Chem. Soc.* **115,** 8706–8715 (1993).
13. Murray, C. B. *et al.* Colloidal synthesis of nanocrystals and nanocrystal superlattices. *IBM J. Res. Dev.* **45,** 47–56 (2001).
14. Klimov, V. I. Optical nonlinearities and ultrafast carrier dynamics in semiconductor nanocrystals. *J. Phys. Chem. B* **104,** 6112–6123 (2000).
15. Klimov, V. I. & McBranch, D. W. Femtosecond 1P-to-1S electron relaxation in strongly confined semiconductor nanocrystals. *Phys. Rev. Lett.* **80,** 4028–4031 (1998).
16. Landsberg, P. T. *Recombination in Semiconductors* (Cambridge Univ. Press, Cambridge, 1991).
17. Klimov, V. I., Mikhailovsky, A. A., McBranch, D. W., Leatherdale, C. A. & Bawendi, M. G. Quantization of multiparticle Auger rates in semiconductor quantum dots. *Science* **287,** 1011–1013 (2000).
18. Achermann, M., Hollingsworth, J. A. & Klimov, V. I. Multiexcitons confined within a subexcitonic volume: Spectroscopic and dynamical signatures of neutral and charged biexcitons in ultrasmall semiconductor nanocrystals. *Phys. Rev. B* **68,** 245302 (2003).
19. Shionoya, H., Saito, H., Hanamura, E. & Akimoto, O. Anisotropic excitonic molecules in CdS and CdSe. *Solid State Commun.* **12,** 223–226 (1973).
20. Htoon, H., Cox, P. J. & Klimov, V. I. Structure of excited-state transitions of individual semiconductor nanocrystals probed by photoluminescence excitation spectroscopy. *Phys. Rev. Lett.* **93,** 187402 (2004).
21. Crooker, S. A., Barrick, T., Hollingsworth, J. A. & Klimov, V. I. Multiple temperature regimes of radiative decay in CdSe nanocrystal quantum dots: Intrinsic limits to the dark-exciton lifetime. *Appl. Phys. Lett.* **82,** 2793–2795 (2003).
22. Wehrenberg, B. L., Wang, C. J. & Guyot-Sionnest, P. Interband and intraband optical studies of PbSe colloidal quantum dots. *J. Phys. Chem. B* **106,** 10634–10640 (2002).
23. Du, H. *et al.* Optical properties of colloidal PbSe nanocrystals. *Nano Lett.* **2,** 1321–1324 (2002).

Acknowledgements

This work was supported by the Chemical Sciences, Biosciences and Geosciences Division of the Office of Basic Energy Sciences, Office of Science, US Department of Energy and Los Alamos LDRD funds. R.D.S. is supported by a Frederick Reines Fellowship. We thank J. M. Pietryga and M. A. Petruska for fabrication of nanocrystal samples.
Correspondence and requests for materials should be addressed to V.I.K.

Competing financial interests

The authors declare that they have no competing financial interests.

Reprints and permission information is available online at http://npg.nature.com/reprintsandpermissions/

©2005 Nature Publishing Group